Monitor Placement for Fault Localization in Deep Neural Network Accelerators

Wei-Kai Liu*, Benjamin Tan†, and Krishnendu Chakrabarty‡
*Duke University, †University of Calgary, ‡Arizona State University
weikai.liu@duke.edu, benjamin.tan1@ucalgary.ca, krishnendu.chakrabarty@asu.edu

***Abstract*—Systolic arrays are a prominent choice for deep neural network (DNN) accelerators because they offer parallelism and efficient data reuse. Improving the reliability of DNN accelerators is crucial as hardware faults can degrade the accuracy of DNN inferencing. Systolic arrays make use of a large number of processing elements (PEs) for parallel processing, but when one PE is faulty, the error propagates and affects the outcomes of downstream PEs. Due to the large number of PEs, the cost associated with implementing hardware-based runtime monitoring of every single PE is infeasible. We present a solution to optimize the placement of hardware monitors within systolic arrays. We first prove that $2N-1$ monitors are needed to localize a single faulty PE and we also derive the monitor placement. We show that a second placement optimization problem, which minimizes the set of candidate faulty PEs for a given number of monitors, is NP-hard. Therefore, we propose a heuristic approach to balance the reliability and hardware resource utilization in DNN accelerators when number of monitors is limited. Experimental evaluation shows that to localize a single faulty PE, an area overhead of only 0.33% is incurred for a 256×256 systolic array.**

I. Introduction

Deep neural networks (DNNs) have witnessed a surge in recent years, outperforming traditional machine learning algorithms and finding applications in diverse fields, including natural language processing, code generation, computer vision, autonomous driving, and more [1]–[5]. To address the intensive computational demands of DNNs, there is growing interest in specialized hardware accelerators for DNNs to enhance performance and energy efficiency [6]–[9]. Many custom ASIC and FPGA accelerators have been proposed to achieve this goal [10]–[13]. For example, Google introduced the tensor processing unit (TPU), a dedicated hardware accelerator that utilizes a systolic array-based approach for matrix multiplication to enable high parallelism in computations [8], [14]. Systolic arrays consist of a grid of processing elements (PEs) communicating exclusively with their neighboring PEs. Every PE performs a multiply-and-accumulate (MAC) operation on incoming data within the array and then forwards the accumulated results downstream. This synchronized data flow throughout the array eliminates the need for input buffering and complex routing mechanisms [15], [16].

However, because of the data-streaming nature of systolic arrays, an erroneous result originating from a single PE will propagate downstream, potentially leading to catastrophic errors or compromising the overall inferencing accuracy [17]–[20]. Several techniques have been proposed to address permanent and transient faults within systolic arrays, including software- and hardware-based solutions. Hardware-based approaches employ redundant PEs to replace faulty PEs [21]–[24]. These methods assume that faults can be localized during testing, thereby assuming that the precise locations of faults are known [17], [21], [23], [25].

Moreover, faults that may elude detection during testing or manifest only during runtime [26]–[28], rendering the aforementioned fault-tolerant techniques ineffective. Even though prior work [18] can obtain test patterns to detect latent defects in the DNN accelerator, it cannot precisely pinpoint the location of faulty PEs. Therefore, many fault-free PEs, classified as being faulty, may have to be isolated from other PEs, resulting in substantial resource wastage. Other hardware-based runtime monitoring designs can identify errors in the systolic array but often demand excessive resources and introduce substantial delays [29], [30]. Existing methods have limitations in precisely localizing faults during runtime. To address these issues, we introduce a monitor design for assessing the integrity of each PE and a heuristic method for monitor placement under resource constraints while minimizing the number of isolated functional PEs. The main contributions of this paper are as follows:

- We formulate the problem of optimally placing a limited number of monitors to minimize the maximum isolation area. We show that this optimization problem is NP-hard.
- We prove that $2N-1$ monitors are necessary and sufficient to uniquely localize any single faulty PE in an $N \times N$ systolic array.
- A heuristic placement approach is proposed to address the problem of including a single faulty PE in a minimized isolation area using fewer than $2N-1$ monitors. We prove that this problem is NP-hard.
- We evaluate the area overhead of the monitor design and analyze resource usage for fault localization for different array sizes.

The paper is organized as follows. Section II provides background on DNN accelerators and the error detection technique. Section III defines the monitor placement problem and analyzes its NP-hard nature. Section IV presents our proposed heuristic algorithm and discuss the experimental results. We conclude in Section V.

II. Background and Motivation

A. Systolic array for DNN acceleration

A DNN is a computational graph comprising many artificial neurons and a hierarchical layer structure. Each neuron performs multiply-and-accumulate operations for different

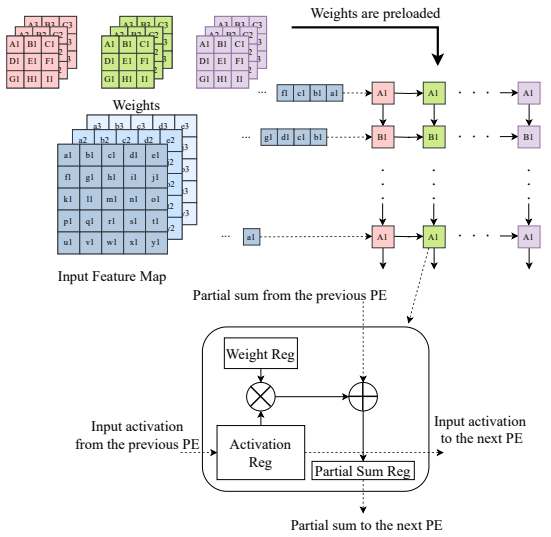

Fig. 1. Systolic array architecture and hardware mapping in weight-stationary dataflow

input data combinations, producing intermediate results that flow to subsequent neuron layers. In this paper, we focus on DNN inference accelerated by systolic arrays. Different DNN-hardware mapping methods are known as dataflows. These dataflows vary in latency, throughput, and data reuse, influencing how inputs and weights are processed and what intermediate results are stored within PEs.

Fig. 1 shows an example of weight stationary dataflow proposed [9]. Here, each weight matrix is allocated to a specific column. Once all the pre-trained weights are loaded into the systolic array, input data is introduced to the PEs from the left and subsequently transferred to the next PE on the right in the next cycle. The partial sums produced in each PE are passed down to the next PE and are aggregated along the assigned column over a total of N cycles to form an output pixel, where N is the number of rows in the array. Once all input features associated with these weights are calculated, new weight matrices are loaded and the process repeats.

DNN acceleration reaps the benefits of data reuse through systolic arrays. However, it also faces the risk of substantial performance degradation when any of the PEs is faulty. Regardless of the chosen dataflow strategy, the interconnected nature of PEs will propagate erroneous values downstream, resulting in incorrect outputs. Furthermore, as different layers of input features and weights are deployed to the same systolic array, the same faulty PEs will be visited repeatedly, significantly undermining the classification accuracy. Previous methods have attempted to address this problem by employing spare PEs for recovery [17], [22]–[25]. However, these approaches assume the location of the faulty PE is already known, without investigating how such localization can be carried out. Therefore, there is a need for a PE-integrity checking solution that can localize faulty PEs during runtime to ensure the reliability and accuracy of DNN acceleration.

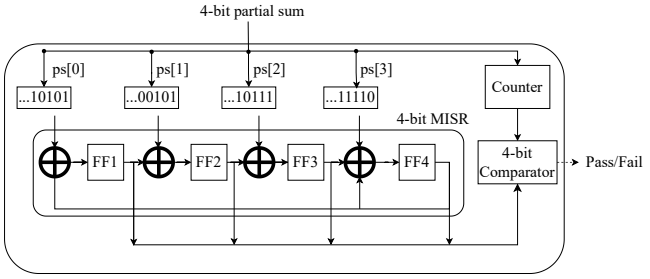

Fig. 2. MISR-based PE monitor design example. This monitor consists of a 4-bit MISR that compresses the PE's partial sum values into a signature, a counter to track the number of cycles, and a comparator to check the final signature against the golden value after the predetermined count.

B. Monitor Design

To detect faults and errors in the computation of each PE, we use a hardware monitoring technique based on Multiple Input Signature Registers (MISRs). MISRs are specialized shift registers that generate signatures representing streams of input data [31], [32].

As shown in Fig. 2, a MISR comprises D flip-flops in a shift register arrangement with additional XOR gates that create feedback. By XORing new data into the current state on each cycle, the MISR state transitions in a way that compresses the inputs into a condensed signature. We apply this to monitor the partial sum values computed by each PE over time. The 4-bit MISR example in Fig. 2 receives the 4-bit partial sum as input on each clock cycle. A counter tracks the number of cycles K that the PE runs for. After K cycles, the comparator checks whether the accumulated MISR signature matches the golden value representing fault-free computation. Any deviation indicates that a hardware fault, design bug, or malicious attack has occurred.

MISR-based monitoring provides an efficient way to compress a long stream of intermediate values into a signature that captures the essence of the computation. By comparing each PE's signature against the golden value, we can rapidly detect errors and faults during accelerator operation. Various sizes of MISR-based monitors are discussed in Section IV.

III. Problem Formulation

We focus on scenarios where a PE is affected by hardware faults, design bugs, or malicious attacks. Without loss of generality, we describe the integrity checking problem for hardware faults. Given an $N \times N$ systolic array, we aim to determine an optimal monitor placement to minimize performance degradation. The monitor (embedded within a PE) serves the purpose of detecting abnormalities in an upstream PE's output. It is important to note that an incorrect output from a PE might not necessarily originate within that PE itself. It could result from errors from other upstream PEs, which are then propagated to the PE under consideration. Consequently, without additional information that can help identify the functional PEs, we must treat any PEs that may contribute to the incorrect output as

TABLE I
PE COVERAGE AREA IN THE 4X4 SYSTOLIC ARRAY

PE	1	2	3	4	5	6	7	8	9	10	11	12	13	14	15	16
1	1	0	0	0	0	0	0	0	0	0	0	0	0	0	0	0
2	1	1	0	0	0	0	0	0	0	0	0	0	0	0	0	0
3	1	1	1	0	0	0	0	0	0	0	0	0	0	0	0	0
4	1	1	1	1	0	0	0	0	0	0	0	0	0	0	0	0
5	1	0	0	0	1	0	0	0	0	0	0	0	0	0	0	0
6	1	1	0	0	1	1	0	0	0	0	0	0	0	0	0	0
7	1	1	1	0	1	1	1	0	0	0	0	0	0	0	0	0
8	1	1	1	1	1	1	1	1	0	0	0	0	0	0	0	0
9	1	0	0	0	1	0	0	0	1	0	0	0	0	0	0	0
10	1	1	0	0	1	1	0	0	1	1	0	0	0	0	0	0
11	1	1	1	0	1	1	1	0	1	1	1	0	0	0	0	0
12	1	1	1	1	1	1	1	1	1	1	1	1	0	0	0	0
13	1	0	0	0	1	0	0	0	1	0	0	0	1	0	0	0
14	1	1	0	0	1	1	0	0	1	1	0	0	1	1	0	0
15	1	1	1	0	1	1	1	0	1	1	1	0	1	1	1	0
16	1	1	1	1	1	1	1	1	1	1	1	1	1	1	1	1

suspects and consider isolating them. The set of isolated PEs constitutes the "isolation area".

The optimization problem addressed in this paper is as follows: *Given m monitors for an $N \times N$ systolic array, determine their optimal placement such that the number of isolated PEs is minimized.*

A. Preliminaries

To formalize this placement problem, we construct a table that outlines the coverage area of each PE, as presented in Table I. The *coverage area* is the region where errors may originate and subsequently be detected by the monitor at the same PE. In this table, the header represents individual PEs, and each index indicates a monitor location. Each row shows the coverage area of each monitor location. Here, 0 (1) signifies that a fault is not detected (detected). For example, in row 6, '1's are assigned to PE1, 2, 5, and 6, implying that a fault originating from one of these PEs can be detected by placing a monitor at PE6; this monitor placement results in an isolation area of 4 because we cannot determine which of the four PEs is faulty. A signature is a sequence of outputs obtained from monitors. When the faulty PE is within the coverage area of a monitor, the monitor will output '1' while others will output '0'. Therefore, multiple scenarios of faulty PEs might lead to the same signature.

B. Fault detection for a specific PE

To localize a faulty PE, it is necessary to position monitors so that a faulty PE can be uniquely identified. Therefore, we first solve the fault detection problem for a specific PE. Consider the case of fault detection at PE11. For us to uniquely identify a fault at PE11, we require a generated signature that is exclusive to PE11 when it is faulty. The generated signature when PE11 is faulty corresponds to the sequence of values in column 11 of Table I, with each value corresponding to a row where a monitor is placed. For instance, three monitors at PE7, 10, and 11 will make faulty PE11 uniquely identifiable as the monitors at PE7 and PE10 report 0 and the monitor at PE11 reports 1. In this configuration, it is impossible to have the signature (001) when the other PE is faulty. Therefore, this signature is exclusively linked to a faulty PE11.

We can frame this problem as a set cover problem to strategically position monitors for detecting a specific faulty PE while minimizing the number of monitors used. The *set cover* problem is defined as follows: given a universal set $\mathbb{U}$ of all elements, along with a set of subsets $S_1, S_2, \ldots, S_k \subseteq \mathbb{U}$, the objective is to choose the fewest number of subsets such that their union covers the universal set [33].

To identify the faulty PE11, we establish a set for each row (monitor location) that includes all the columns (PEs) with different values in Table I from column 11 (PE11). We aim to identify these sets so that their union forms the universal set, ensuring that every PE has at least one distinct outcome from the selected monitors compared to PE11. The universal set is the union of all the subsets. The following sets are established:
$Set_1 = \{1\}$, $Set_2 = \{1, 2\}$, ...
$Set_7 = \{1, 2, 3, 5, 6, 7\}$, $Set_8 = \{1, 2, 3, 4, 5, 6, 7, 8\}$,
$Set_9 = \{1, 5, 9\}$, $Set_{10} = \{1, 2, 5, 6, 9, 10\}$,
$Set_{11} = \{4, 8, 12, 13, 14, 15, 16\}$,
$Set_{12} = \{13, 14, 15, 16\}$, $Set_{13} = \{1, 5, 9, 13\}$,
$Set_{14} = \{1, 2, 5, 6, 9, 10, 13, 14\}$,
$Set_{15} = \{4, 8, 12, 16\}$, $Set_{16} = \{\}$,
$\mathbb{U} = \{1, 2, 3, 4, 5, 6, 7, 8, 9, 10, 12, 13, 14, 15, 16\}$

Lemma 1. *For any given PE, PEi, a solution to the set cover problem can uniquely identify a fault in PEi.*

Proof. For a given monitor location PEj, we construct a set Set_j containing all PEs that will produce a different monitor output compared to PEi when faulty. Specifically, Set_j includes PEs that will cause the monitor at PEj to output a distinct value of 0 or 1 when faulty, as opposed to the value of 1 or 0 that would be observed if PEi was faulty instead. Our goal is to find the minimum set of monitor locations that can uniquely identify a fault at PEi. This can be achieved by ensuring that for every other PE, there is at least one monitor that produces a distinct output compared to PEi when faulty. Therefore, a solution to the set cover problem provides the minimum number of monitor locations to ensure that each PE has at least one distinct output from these monitors compared to PEi when they are faulty. This, in turn, results in a unique signature when PEi is faulty using the fewest monitors. □

In our example, when we solve the fault localization problem for PE11, four solutions are found:

1) (Set_7, Set_{10}, Set_{11}),
2) (Set_7, Set_{11}, Set_{14}),
3) (Set_8, Set_{10}, Set_{11}),
4) (Set_8, Set_{11}, Set_{14}).

Each solution shows the PEs where monitors should be placed so that faulty PE11 can be identified with the minimum number of monitors. These solutions are illustrated in Fig. 3(a), where PE11 is always selected, and we have to select one PE each from the blue and green rectangles for monitor placement. As we outline the coverage area of each monitor location in Fig. 3(b), the PEs associated with different signatures are naturally separated by the dotted lines. For instance, we can observe that PE11 is enclosed within the red rectangle, while

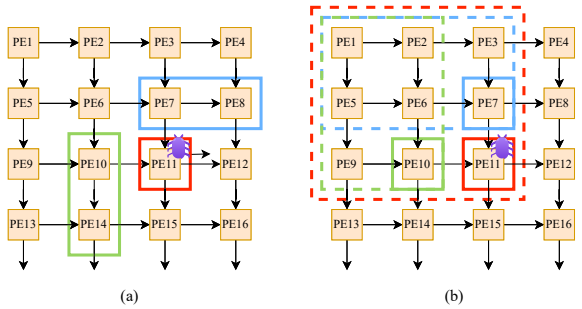

Fig. 3. A 4×4 systolic array. Solid rectangles highlight the locations of monitors, and the faulty PE, marked with a purple bug, represents the faulty PE. Dotted rectangles outline the coverage area of each monitor. (a) displays the solution set for detecting the faulty PE11, and (b) visualizes distinct groups of PE when different signatures are reported.

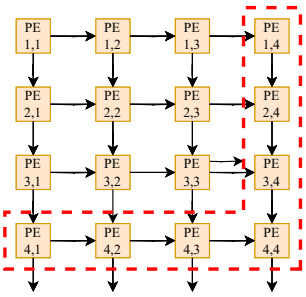

Fig. 4. Optimal monitor placement for single faulty PE localization

neither the blue nor the green rectangles encompass PE11. This scenario corresponds to the signature (001) generated by monitors placed on PE7, 10, and 11, respectively, when PE11 is faulty.

C. Localizing a single faulty PE

Since the faulty PE can be located anywhere in this 4×4 array, localizing the faulty PE becomes equivalent to solving 16 set cover problems simultaneously – one for each possible PE location. We define this as the **integrated set cover problem**. In this formulation, the 16 set cover problems are coupled rather than independent, as selecting a monitor placement impacts the subset selection across all set cover instances. Specifically, monitor placement for PEi involves simultaneous selection of monitoring subsets in all 16 problems.

We define the integrated set cover problem as follows: Let $U = \{U_1, U_2, \ldots, U_{N^2}\}$ be the collection of universal sets, where each U_i corresponds to the universal set of the set cover problem for PEi. For each U_i, let $S_i = \{S_i^1, S_i^2, \ldots, S_i^{N^2}\}$ be the collection of subsets for PEi, which can be constructed following the method described in Section III-B. Let $I = \{InS^1, InS^2, \ldots, InS^{N^2}\}$ be the collection of integrated sets, where $InS^j = \{S_1^j, S_2^j, \ldots, S_{N^2}^j\}$ contains the j^{th} subset from each S_i. Find a minimum subset $C \subseteq I$ such that:

$$\bigcup_{InS^j \in C} S_i^j = U_i, \forall i \in 1, 2, \ldots, N^2, \tag{1}$$

i.e., we want to pick the smallest set of integrated sets whose chosen subsets collectively cover every universal set U_i. This set can localize any single-fault PE.

We next prove that optimal monitor placement for localizing any single faulty PE in an $N \times N$ systolic array corresponds to $2N - 1$ monitors positioned along the array boundaries. This structured boundary placement, as illustrated in Fig. 4, generates unique signatures for each faulty PE.

Lemma 2. *(Sufficient Condition) In an $N \times N$ systolic array, placing $2N - 1$ monitors at locations $PE_{i,N}$ and $PE_{N,j}$ for $1 \leq i, j \leq N$ can localize any single faulty PE.*

Proof. For a faulty $\text{PE}_{i,j}$, $1 \leq i, j \leq N$, we can identify the monitors required to create a unique signature for it. Below are the monitor locations and the corresponding outcomes for localizing the faulty $\text{PE}_{i,j}$ when i and j vary.

1) If $i \neq 1$ and $i \neq N$ and $j \neq 1$ and $j \neq N$:
($\text{PE}_{i-1,N}$, $\text{PE}_{N,j-1}$, $\text{PE}_{i,N}$, $\text{PE}_{N,j}$), (0,0,1,1)
2) If ($i = N$ or $j = N$) and ($i \neq 1$ and $j \neq 1$):
($\text{PE}_{i-1,N}$, $\text{PE}_{N,j-1}$, $\text{PE}_{i,j}$), (0,0,1)
3) If $i = 1$ and $j \neq 1$:
($\text{PE}_{N,j-1}$, $\text{PE}_{1,N}$, $\text{PE}_{N,j}$), (0,1,1)
4) If $i \neq 1$ and $j = 1$:
($\text{PE}_{i-1,N}$, $\text{PE}_{i,N}$, $\text{PE}_{N,1}$), (0,1,1)
5) If $i = 1$ and $j = 1$:
($\text{PE}_{1,N}$, $\text{PE}_{N,1}$), (1,1)

Since there is a 1-to-1 mapping from signatures to the faulty PE at any position, we can localize any single faulty PE. □

Lemma 3. *(Necessary Condition) Monitors at locations $PE_{i,N}$ and $PE_{N,j}$ for $1 \leq i, j \leq N$ are necessary to localize some faulty PEs in an $N \times N$ systolic array.*

Proof. The monitors at $\text{PE}_{i,N}$ for $1 \leq i \leq N-1$ are needed to localize $\text{PE}_{i,N}$, since no other location distinguishes it from $\text{PE}_{i+1,N}$. This can be proved by constructing the set cover problem for $\text{PE}_{i,N}$, and analyzing the subsets. The union of all sets excluding $Set_{i,N}$ will not cover the entire universal set, implying that the monitor at $\text{PE}_{i,N}$ is necessary for localizing $\text{PE}_{i,N}$. Similarly, monitors at $\text{PE}_{N,j}$ for $1 \leq j \leq N-1$ are required for $\text{PE}_{N,j}$. Lastly, a monitor at $\text{PE}_{N,N}$ is needed for itself. Thus, the stated monitor placements are necessary for localizing some PEs. □

We now state the following key result.

Theorem 1. *Placing $2N-1$ monitors at locations $PE_{i,N}$ and $PE_{N,j}$ for $1 \leq i, j \leq N$ provides an optimal solution for the integrated set cover problem for localizing a single faulty PE in an $N \times N$ array.*

Proof. Based on the sufficiency from Lemma 2 and necessity from Lemma 3, we can conclude that $2N-1$ monitors along the boundaries is an optimal placement. □

D. Minimizing the maximum isolation area

Having proven that each faulty PE can be precisely localized by employing $2N-1$ monitors, when dealing with a large systolic array, such as 256×256 PEs in the Google Tensor Processing Unit (TPU), allocating 511 monitors is a significant resource investment. To trade off resource investment with the effectiveness of fault localization, we now try to minimize the isolation area given a limited number of monitors. Recall that the isolation area is the set of PEs that cannot be distinguished from the faulty PE using the monitors. Consider a 4×4 array with monitors placed at PE7, 10, and 11, as shown in Fig. 3(b). Five groups are generated based on five possible signatures.

1) (111): {PE1, PE2, PE5, PE6}
2) (101): {PE3, PE7}
3) (011): {PE9, PE10}
4) (001): {PE11}
5) (000): {PE4, PE8, PE12, PE13, PE14, PE15, PE16}

The PEs in the same group produce identical signatures if any PE in the group becomes faulty. In this configuration, the maximum isolation area is 7, i.e., 7 PEs will be isolated when one PE in group 5 becomes faulty. A larger isolation area means more PEs are grouped and indistinguishable when faults occur. This reduces the precision of locating the faulty PE, which impacts processing capabilities and reduces inferencing performance. It is crucial to minimize the isolation area to minimize the number of candidate faulty PEs and maintain high throughput after the isolated PEs are no longer available.

Thus, we formulate the **Optimal Monitor Placement Problem**: Given an $N \times N$ systolic array and m available monitors, find the monitor placement that minimizes the isolation area. Importantly, at least one monitor must be positioned at $\text{PE}_{N,N}$ to observe faults from downstream PEs. Additional monitors can then be strategically placed to refine fault localization.

Theorem 2. *The Monitor Placement Optimization Problem (MPOP) is NP-hard.*

Proof. We first show that the integrated set cover problem, which is NP-hard, is a special case of MPOP. The NP-hardness of the integrated set cover problem can be demonstrated via a polynomial time reduction from the original set cover problem. In the set cover problem, given a universal set $\mathbb{U}$ and subsets $S_1, \ldots, S_k \subseteq \mathbb{U}$, the goal is to find the smallest subcollection that covers $\mathbb{U}$. To reduce this to the integrated set cover problem, we construct k collections of k identical sets, $InS^1, \ldots, InS^k$, where each InS^i contains subsets $InSubset^i_j = S_i$ for $1 \leq j \leq k$. A solution to the original problem maps to the same indexed integrated sets. Now, consider modeling the integrated set cover instance as the MPOP. By incrementally adding monitors m until the isolation area reaches 1, we can solve the integrated set cover problem. Therefore, the MPOP generalizes the integrated set cover problem. Since the integrated set cover problem is NP-hard, the more general MPOP is also NP-hard. □

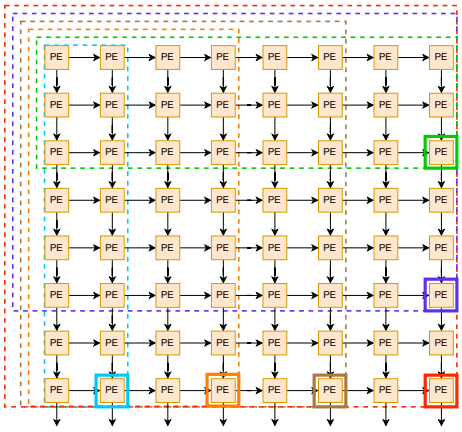

Fig. 5. A monitor placement generated by our heuristic for a 10×10 array with 6 monitors results in an isolation area of 6, distinguished by different colors. The solid rectangles indicate the monitor locations, while the dotted rectangles represent the coverage area of each monitor.

Algorithm 1 Heuristic for MPOP

Input: N, $m > 2$
// size of the systolic array, number of monitors
Output: $Area$, $placement$

$m \leftarrow m - 1$;
$Map \leftarrow \{\}$;
$isolation\_area \leftarrow []$;
$combinations \leftarrow []$;
for i:=1 **to** $\lfloor (\frac{m}{2}) \rfloor$ **do**
  $combinations \leftarrow (i+1, m-i+1)$
end for
for $(right\_num, bottom\_num)$ in $combinations$ **do**
  $right \leftarrow \lceil (\frac{N}{right\_num}) \rceil$;
  $bottom \leftarrow \lceil (\frac{N}{bottom\_num}) \rceil$;
  $isolation\_area.insert(right \times bottom)$;
end for
$Area \leftarrow min(isolation\_area)$;

IV. Heuristic Solution and Experimental Results

A. Proposed heuristic

To solve MPOP, we propose a heuristic to minimize the maximum isolation area, as shown in Algorithm 1. Since the monitors in an optimal placement when $m = 2N-1$ are located on the rightmost column and the bottommost row, our heuristic places the monitors on these two borders and traverses the possible outcomes for the minimized isolation area. Specifically, the heuristic first generates all combinations of (i, j), $0 < i \leq j < m$, to separate monitors on the right and bottom borders. It then places monitors along each border with equal spacing if possible. An example solution using our heuristic is shown in Fig. 5, where there are 4 monitors with spacing 2 on the bottom and 3 monitors with spacing (3,3,2). By generating all valid (i, j) combinations and placing the monitors evenly along the borders, the heuristic finds the minimum isolation area given the constraint that the monitors must be placed on the borders.

Table II compares optimal solutions obtained through brute force search for smaller values of N and m and our heuristic. The computational complexity of brute force search in this problem is $O(N^{2m})$, making it infeasible for larger N. In contrast, the computational complexity of our heuristic is $O(m)$.

TABLE II

THE ISOLATION AREA COMPARISON BETWEEN THE OPTIMAL SOLUTION AND OUR HEURISTIC IN DIFFERENT SCENARIOS. "-" INDICATES THE INFEASIBILITY OF DERIVING THE OPTIMAL SOLUTION THROUGH BRUTE FORCE SEARCHING. "*" INDICATES THE SCENARIOS WHERE OUR HEURISTIC LEADS TO THE OPTIMAL SOLUTION.

m	N=4		N=5		N=6		N=7		N=8		N=9		N=10	
	Optimal	Heuristic	Optimal	Heuristic	Optimal	Heuristic	Optimal	Heuristic	Optimal	Heuristic	Optimal	Heuristic	Optimal	Heuristic
1	16*	16*	25*	25*	36*	36*	49*	49*	64*	64*	81*	81*	100*	100*
2	8	8	13	13	18	18	25	28	32	32	41	45	50	50
3	4*	4*	8	9	9*	9*	15	16	16*	16*	24	25	25*	25*
4	4	4	5	6	6	6	9	12	12	12	15	15	20	20
5	2	2	4	4	4*	4*	6	8	8	8	9*	9*	12	15
6	2	2	3	3	4	4	5	6	6	6	8	9	9	10
7	1*	1*	2	2	3	3	4	4	4*	4*	6	6	8	8
8			2	2	2	2	4	4	4	4	5	6	6	6
9			1*	1*	2	2	3	3	4	4	4	4	4*	4*
10					2	2	2	2	3	3	-	4	-	4
11					1*	1*	2	2	2	2	-	3	-	4
12							2	2	2	2	-	3	-	4
13							1*	1*	2	2	-	2	-	3
14									2	2	-	2	-	2
15									1*	1*	-	2	-	2
16											-	2	-	2
17											1*	1*	-	2
18													-	2
19													1*	1*

TABLE III

AREA OVERHEAD FOR VARIOUS MONITOR PLACEMENTS, ALONG WITH THE MAXIMUM SIZE OF ISOLATION AREA GENERATED BY OUR HEURISTIC IN DIFFERENT SCENARIOS.

Array size (N)	Number of monitors (m)	Isolation area size	Synthesized area (% systolic array) 24-bit	Synthesized area (% systolic array) 32-bit
256	511	1	0.36%	0.45%
256	383	2	0.27%	0.34%
256	255	4	0.18%	0.23%
128	255	1	0.72%	0.90%
128	191	2	0.36%	0.45%
128	63	4	0.18%	0.22%
64	127	1	1.44%	1.80%
64	95	2	1.08%	1.35%
64	31	4	0.35%	0.44%
32	63	1	2.86%	3.57%
32	47	2	2.14%	2.66%
32	15	4	0.68%	0.85%

While we only show the process of finding the isolation area for simplicity, the monitor placement can be easily derived through a similar process. We observe that our heuristic finds the optimal solution when:

$$N \equiv 0 \pmod{\frac{m+1}{2}}, \tag{2}$$

as marked with asterisks in the table. This ensures equal monitor counts on both borders with equal spacing. Intuitively, this symmetry enables minimizing the maximum isolation area. For other scenarios, our heuristic still provides near-optimal placements, significantly reducing search complexity. Overall, it delivers an efficient and effective approach for monitor placement for fault localization.

B. Area Overhead

We evaluate the area overhead of monitors for different systolic array sizes and monitor numbers. Table III shows the overhead results and maximum isolation area achieved by our heuristic. The PE and monitor are synthesized with Synopsys DC using a 45 nm library.

We implement two PE designs for comparison. The first design following the TPU design from [18], with 8-bit weights/activations, 16-bit multipliers, and 24-bit accumulators. Its corresponding monitor employs a 24-bit MISR, tailored to match the partial sum width. The second design, which is from [8], employs 32-bit accumulators, leading to the synthesis of a 32-bit MISR monitor. This results in PE-level area overheads of 46.5% and 58% for the two monitors, corresponding to the first and second PE designs, respectively. The disparity in overhead arises from the larger width of the second MISR, despite identical weights and multipliers in both PE designs. While the design and implementation of the monitor is not the primary focus of this work, analyzing the area overhead of these monitors serves as a reference point for understanding the resource utilization of PE fault-checking designs. At the array level, then area overhead due to the monitors is negligible, less than 1% in most cases.

In Table III, we set array sizes to common TPU values (256, 128) and smaller sizes for comparison. To precisely localize the faulty PE, we set the $m = 2N-1$. Based on our heuristic, we derive monitor placements that achieve isolation areas of 2 and 4 when $m = \frac{3N}{2} - 1$ and $N - 1$, respectively. We analyze the resource usage of each placement compared to the synthesized systolic array area, which consists of PEs with 24-bit and 32-bit accumulators. For simplicity, we estimate systolic array area by multiplying the number of PEs by the area of a PE, ignoring interconnections and I/O buffers. Note that this assessment overestimates the area overhead.

Table III indicates that achieving the same isolation area requires higher resource utilization for smaller array sizes. Conversely, for larger values of N, such as 256, the additional area overhead required to achieve an isolation area of one becomes negligible. Even with the higher monitor area in the 32-bit systolic array, it still incurs less than 0.5% of the entire systolic array area.

V. CONCLUSIONS

We have presented an optimization method to optimize the placement of hardware monitors for fault localization in systolic array-based DNN accelerators. We have formulated

the monitor placement problem under resource constraints and proved that it is NP-hard. We also proved that $2N-1$ monitors along the boundaries of an $N \times N$ array is optimal for the unique localization of a single faulty PE, , when no constraint is imposed on the number of monitors.. To reduce the overhead incurred by monitors, we proposed a heuristic to minimize the maximum isolation area with a limited number of monitors. Our overhead analysis shows that, only 0.36% additional area overhead is required to localize a single faulty PE in a 256×256 systolic array. As part of future work, we will extend this method to handle multiple faulty PEs.

REFERENCES

[1] W. Yin, K. Kann, M. Yu, and H. Schütze, "Comparative study of CNN and RNN for natural language processing," *arXiv preprint arXiv:1702.01923*, 2017.

[2] P. Nagrath, R. Jain, A. Madan, R. Arora, P. Kataria, and J. Hemanth, "Ssdmnv2: A real time DNN-based face mask detection system using single shot multibox detector and mobilenetv2," *Sustainable Cities and Society*, 2021.

[3] A. E. Sallab, M. Abdou, E. Perot, and S. Yogamani, "Deep reinforcement learning framework for autonomous driving," *arXiv preprint arXiv:1704.02532*, 2017.

[4] S. P. Singh, A. Kumar, H. Darbari, L. Singh, A. Rastogi, and S. Jain, "Machine translation using deep learning: An overview," in *International Conference on Computer, Communications and Electronics (Comptelix)*, 2017.

[5] H. Pearce, B. Ahmad, B. Tan, B. Dolan-Gavitt, and R. Karri, "Asleep at the keyboard? assessing the security of github copilot's code contributions," in *IEEE Symposium on Security and Privacy (SP)*, 2022.

[6] M. Alwani, H. Chen, M. Ferdman, and P. Milder, "Fused-layer CNN accelerators," in *IEEE/ACM International Symposium on Microarchitecture (MICRO)*, 2016.

[7] T. Chen, Z. Du, N. Sun, J. Wang, C. Wu, Y. Chen, and O. Temam, "Diannao: A small-footprint high-throughput accelerator for ubiquitous machine-learning," *ACM SIGARCH Computer Architecture News*, 2014.

[8] N. P. Jouppi, C. Young, N. Patil, D. Patterson, G. Agrawal, R. Bajwa, S. Bates, S. Bhatia, N. Boden, A. Borchers *et al.*, "In-datacenter performance analysis of a tensor processing unit," in *Proceedings of International Symposium on Computer Architecture*, 2017.

[9] Y.-H. Chen, J. Emer, and V. Sze, "Eyeriss: A spatial architecture for energy-efficient dataflow for convolutional neural networks," *ACM SIGARCH Computer Architecture News*, 2016.

[10] S. K. Venkataramanaiah, S. Yin, Y. Cao, and J.-S. Seo, "Deep neural network training accelerator designs in ASIC and FPGA," in *International SoC Design Conference (ISOCC)*, 2020.

[11] R. Machupalli, M. Hossain, and M. Mandal, "Review of ASIC accelerators for deep neural network," *Microprocessors and Microsystems*, 2022.

[12] L. Yang, Z. Yan, M. Li, H. Kwon, L. Lai, T. Krishna, V. Chandra, W. Jiang, and Y. Shi, "Co-exploration of neural architectures and heterogeneous ASIC accelerator designs targeting multiple tasks," in *ACM/IEEE Design Automation Conference (DAC)*, 2020.

[13] Y. Hu, Y. Liu, and Z. Liu, "A survey on convolutional neural network accelerators: GPU, FPGA and ASIC," in *International Conference on Computer Research and Development (ICCRD)*, 2022.

[14] L. Jia, L. Lu, X. Wei, and Y. Liang, "Generating systolic array accelerators with reusable blocks," *IEEE Micro*, 2020.

[15] A. Samajdar, Y. Zhu, P. Whatmough, M. Mattina, and T. Krishna, "Scale-sim: Systolic CNN accelerator simulator," *arXiv preprint arXiv:1811.02883*, 2019.

[16] K. Johnson, A. Hurson, and B. Shirazi, "General-purpose systolic arrays," *Computer*, 1993.

[17] J. J. Zhang, K. Basu, and S. Garg, "Fault-tolerant systolic array based accelerators for deep neural network execution," *IEEE Design & Test*, 2019.

[18] S. Kundu, S. Banerjee, A. Raha, S. Natarajan, and K. Basu, "Toward functional safety of systolic array-based deep learning hardware accelerators," *IEEE Transactions on Very Large Scale Integration (VLSI) Systems*, 2021.

[19] G. Li, S. K. S. Hari, M. Sullivan, T. Tsai, K. Pattabiraman, J. Emer, and S. W. Keckler, "Understanding error propagation in deep learning neural network (DNN) accelerators and applications," in *Proceedings of the International Conference for High Performance Computing, Networking, Storage and Analysis*, 2017.

[20] J. Tan, Q. Wang, K. Yan, X. Wei, and X. Fu, "Saca-FI: A microarchitecture-level fault injection framework for reliability analysis of systolic array based CNN accelerator," *Future Generation Computer Systems*, 2023.

[21] K. Cho, I. Lee, H. Lim, and S. Kang, "Efficient systolic-array redundancy architecture for offline/online repair," *Electronics*, 2020.

[22] I. Takanami and M. Fukushi, "A built-in circuit for self-repairing mesh-connected processor arrays with spares on diagonal," in *IEEE Pacific Rim International Symposium on Dependable Computing (PRDC)*, 2017.

[23] Y. Zhao, K. Wang, and A. Louri, "FSA: An efficient fault-tolerant systolic array-based DNN accelerator architecture," in *IEEE International Conference on Computer Design (ICCD)*, 2022.

[24] Y.-C. Chang, C.-T. Chiu, S.-Y. Lin, and C.-K. Liu, "On the design and analysis of fault tolerant NoC architecture using spare routers," in *Asia and South Pacific Design Automation Conference (ASP-DAC)*, 2011.

[25] J. J. Zhang, T. Gu, K. Basu, and S. Garg, "Analyzing and mitigating the impact of permanent faults on a systolic array based neural network accelerator," in *IEEE VLSI Test Symposium (VTS)*, 2018.

[26] M. A. Hanif and M. Shafique, "Dependable deep learning: Towards cost-efficient resilience of deep neural network accelerators against soft errors and permanent faults," in *International Symposium on On-Line Testing and Robust System Design (IOLTS)*, 2020.

[27] U. S. Solangi, M. Ibtesam, M. A. Ansari, J. Kim, and S. Park, "Test architecture for systolic array of edge-based AI accelerator," *IEEE Access*, 2021.

[28] F. Libano, P. Rech, and J. Brunhaver, "Efficient error detection for matrix multiplication with systolic arrays on FPGAs," *IEEE Transactions on Computers*, 2023.

[29] B. Tan, R. Elnaggar, J. M. Fung, R. Karri, and K. Chakrabarty, "Toward hardware-based IP vulnerability detection and post-deployment patching in systems-on-chip," *IEEE Transactions on Computer-Aided Design of Integrated Circuits and Systems*, 2020.

[30] W.-K. Liu, B. Tan, J. M. Fung, R. Karri, and K. Chakrabarty, "Hardware-supported patching of security bugs in hardware IP blocks," *IEEE Transactions on Computer-Aided Design of Integrated Circuits and Systems*, 2022.

[31] B. Keller and T. Bartenstein, "Use of MISRs for compression and diagnostics," in *IEEE International Conference on Test*, 2005.

[32] C. Barnhart, V. Brunkhorst, F. Distler, O. Farnsworth, B. Keller, and B. Koenemann, "Opmisr: The foundation for compressed ATPG vectors," in *Proceedings of International Test Conference*, 2001.

[33] U. Feige, "A threshold of ln n for approximating set cover," *Journal of the ACM (JACM)*, 1998.